Rock weathering: The effects of varying rock moisture on controlled weathering cycles in low porosity limestone

Andrew Mitchell [*], Oliver Sass

University of Bayreuth, Germany

ABSTRACT

Examples of rockwall weathering processes include diurnal heating and cooling, diurnal and seasonal freezing, wetting and drying and thawing/seasonal active-layer thawing. These stress-loading processes often occur synergistically and cause a weakening of the rockwall through the propagation of sub-critical cracks. The Acoustic Emissions (AE) released by these cracking events can be measured in order to quantify the weathering efficacy. While the effects of thermal cycling are well studied, rock moisture content and its control on these weathering processes is rarely considered in detail.

To better understand rock moistures effect on weathering processes we subjected Wetterstein limestone samples with different starting moisture contents (0 %, 25 %, 50 %, 75 %, 100 %) to thermal cycling above (5 to 35 °C) and below (5 to −10 °C) freezing and a longer freezing cycle with gradual stepped thawing (10 to −10 °C). In addition to this we simulated wetting and drying cycles at a constant temperature. For all of these weathering cycles, relative efficacy was assessed by amount of AE hits and change in effective porosity.

Rock moisture was found to have little effect on the overall AE count and effective porosity increase over shorter thermal cycling. However, freeze-thaw cycling was shown to have similar weathering effect to thermal cycling of 3 K greater thermal gradient above freezing. Meanwhile longer duration freezing cycles see an increase of rock moisture create 4× as many cracking events compared to dry samples. More re-freezing events are seen in lower saturation samples and when considered with the synergistic effects of wetting and drying in natural open systems, the presence and mobility of pore water are considered to be more important than the quantity.

1. Introduction

The breakdown of rocks by weathering is the first step of alpine rock slope erosion (Gilbert, 1877). There are many weathering processes involved in this preparatory weakening of the rockwall, often influenced by meteorological conditions and lithology (Hall, 2013). Examples of such processes include diurnal heating and cooling (Collins and Stock, 2016; Collins et al., 2018), diurnal and seasonal freezing (Matsuoka, 2008), wetting and drying (Sass, 2005; Zhang et al., 2015) and thawing/ seasonal active-layer thawing (Draebing et al., 2017). As all these processes occur simultaneously in nature, the conceptual framework of freeze-thaw weathering in cold regions has repeatedly been questioned (Hall et al., 2002) and the relative importance of interacting processes is still to be determined.

The aforementioned stress-loading processes can cause the propagation of microcracks (Aldred et al., 2016; Eppes et al., 2016) and eventual coalescence to form macrocracks, weakening the rockwall (Cox

and Meredith, 1993; Maji and Murton, 2021) and so making the triggering of rockfall more likely (Collins and Stock, 2016). This subcritical cracking causes measurable acoustic emissions (AE) (Hallet et al., 1991; Eppes and Keanini, 2017). An AE is a transient elastic wave created by the rapid release of energy, such as from crack nucleation, which then propagates inside the material (Lockner, 1993). Once this wave reaches the surface of a material the motion can be detected using an AE sensor, directly attached to the surface, which contains a piezoelectric element (Beattie, 1983). The transducer detected signal, in the low ultrasonic frequency range (10–2000 kHz) (Maji and Murton, 2021), is then converted to an electrical signal. This signal is then generally amplified by a pre-amplifier and a main amplifier due to the signal being weak (Grosse et al., 2022). Finally, the signal is split into discrete waveforms, the characteristics of which can be used to determine features such as energy, cracking mode and source location of the cracking event (Ohno and Ohtsu, 2010; Aggelis, 2011; Grosse et al., 2022; Goszczyńska, 2014).

Previous laboratory experiments in the area of rock weathering have

measured AE activity in both stable thermal boundary conditions (Duca et al., 2014; Hallet et al., 1991) and more recently under dynamic thermal boundary conditions (Maji and Murton, 2021). The field of engineering geology has also performed extensive testing of AE activity on concrete and rocks under single and cyclic loading conditions (Grosse et al., 2022), but the effect of moisture is also rarely considered beyond oven dry and fully saturated samples. Of those studies that do consider the effect of complete saturation on weathering effect, higher porosity samples such as sandstones (C. Li et al., 2021) and tuffs (Dong et al., 2022) were used, but the combined effects of rock moisture levels and temperature cycles have not been considered. These lithologies have completely different porosity style and mechanical properties to the fracture dominated, low percent porosity seen commonly in high mountain/rockwall sites and so require further investigation.

To further understand the role of rock moisture in weathering processes is important as it plays a key role as a limiting factor in mechanical weathering (Hall, 2013), though as pointed out by Sass (2005) it is often not given the same attention as temperature, as there is no single humidity sensor that satisfies all requirements for application in rock. Just the presence of rock moisture in fractures of Carrara marble was shown by Voigtländer et al. (2018) to increase subcritical stress by an order of magnitude. Also, the stresses that swelling and shrinkage of rocks caused by wetting/drying are comparable to strong thermal fluctuations (Hall, 2013), with the expansion caused by hydration alone having been shown in laboratory experiments (Hamès et al., 1987; Prick, 1995; Zhang et al., 2015) to sometimes reach comparable orders of magnitude to that seen in thermal expansion.

Frost weathering laboratory studies by Walder and Hallet (1986) show minimum effective saturations for volumetric ice expansion at over 91 % pore space saturation. This level of saturation is however rarely seen in field measurements for intact rock (Rode et al., 2016; Sass, 2005). More recent studies by Jia et al. (2015) suggest that weathering caused by volumetric expansion could occur at saturations of as low as 50 %, but White (1976) questions how often rocks in mountain areas ever become >50 % saturated followed by rapid freezing, so questioning the efficacy of the process as a whole. For ice segregation, another frost weathering process thought to promote rock breakdown (Walder and Hallet, 1985), defined water saturation thresholds in natural rock are scarce. These vary from 58 % to 65 % (Prick, 1997; Murton et al., 2006. respectively) and are also dependant on lithology. Further to this, as all critical saturation points mentioned are derived from intact rock and are invalid when compared to a fractured rock, where water can concentrate in fractures (Matsuoka, 2001).

With such a disparity between suggested saturations for processes and those often seen in the field, combined with the lithological dependence of these saturation limits it is timely to further investigate how different percentages of rock moisture saturation affect the efficacy of weathering. This study is part of the DfG funded "ClimRock" project which seeks to characterize rockwall weathering from microclimate, rock moisture and rockfall activity. The project follows a conceptual multiscale model integrating the elevation and aspect dependant factors of temperature and moisture gradients in alpine rockwalls, with the aim of improving our understanding of the weathering processes driven by

these factors. Our objective in this laboratory study is to compare how different rock moisture levels affect the efficacy of different weathering processes seen in alpine environments. To achieve this, we have run temperature cycles of differing duration, above and below freezing at different moisture contents and performed diurnal wetting/drying cycles. During the experimental runs we monitored acoustic emissions (AE) generated by microcracking activity as a proxy for the weathering effect on the rock samples. Our aims are summarised as follows:

- to assess the effectiveness of different weathering processes relative to each other in low-porosity rock;
- to assess the role of saturation thresholds for the efficiency of crack formation.

2. Materials and methods

2.1. Rock samples

The field sites of the ClimRock project are in the Northern European Alps near the German-Austrian border. The "Dachstein" and "Dammkar" sites are characterised by steep rockwall built of carbonatic rock of the Wettersteinkalk and Dachsteinkalk formation. We used 10 cm^3 cubes samples of Wetterstein limestone in our laboratory work. The small size is to ensure, as well as possible, that they can be adjusted to an even distribution of rock moisture. The samples were sawn at Hafnach quarry, Flintsbach, Bavaria from the same block of Wetterstein limestone to ensure similar stress history in all the samples. Once transported to University of Bayreuth they were stored in the same storage room with temperature 19 °C ± 0.6 °C and average humidity of 75 % ± 6 %.

For each temperature cycle run the blocks moisture content was controlled by weight. 0 % sample weight was calculated by oven drying at 60 °C until weight change stops. This temperature was chosen to remove the available free water while not causing too much thermal stress. Full sample saturation was achieved by gradual submersion in deionized water until no weight change was observed. The rock samples have an effective porosity range of 0.43 % to 1.74 % (seen in Table 1. below).

The different temperature cycles were performed at 0 %, 25 %, 50 %, 75 % and 100 % rock moisture saturation. It should be noted that for example the "0 %" sample runs in all probability still contain some interstitial pore water which could have been driven out using higher temperatures at the risk of causing thermal cracking. The order of moisture content and temperature cycle for each sample was done at random to ensure minimised impact of progressive weathering effects on experiment outcome.

2.2. Experiment procedure

In order to test the effect of rock moisture during different temperature cycles and wet/dry cycles in a way relatable to the field, experiments with similar temperature ranges and slopes to that seen in an alpine environment were designed.

Short fluctuating temperature cycles (940 min length) between 5 °C

Table 1
Effective porosities of 10 cm^3 Wetterstein limestone samples used in temperature and wet/dry cycles.

Weathering cycle	Warming/cooling (5 to 35 °C @ 6 °C/h)			Freeze/thaw (5 to −10 °C @ 3 °C/h)			Long freeze (10 to −10 °C with staged thawing)			Wet/dry (Air 30 °C, 90 to 20Rh)		
Sample name	W/C1	W/C2	W/C3	F/T1	F/T2	F/T3	LF1 (0 %)	LF2 (50 %)	LF3 (100 %)	W/D1	W/D2	W/D3
Effective porosity (% vol.)	0.43	0.80	0.67	1.10	0.56	1.74	0.54	1.39	0.64	1.1	0.73	0.68
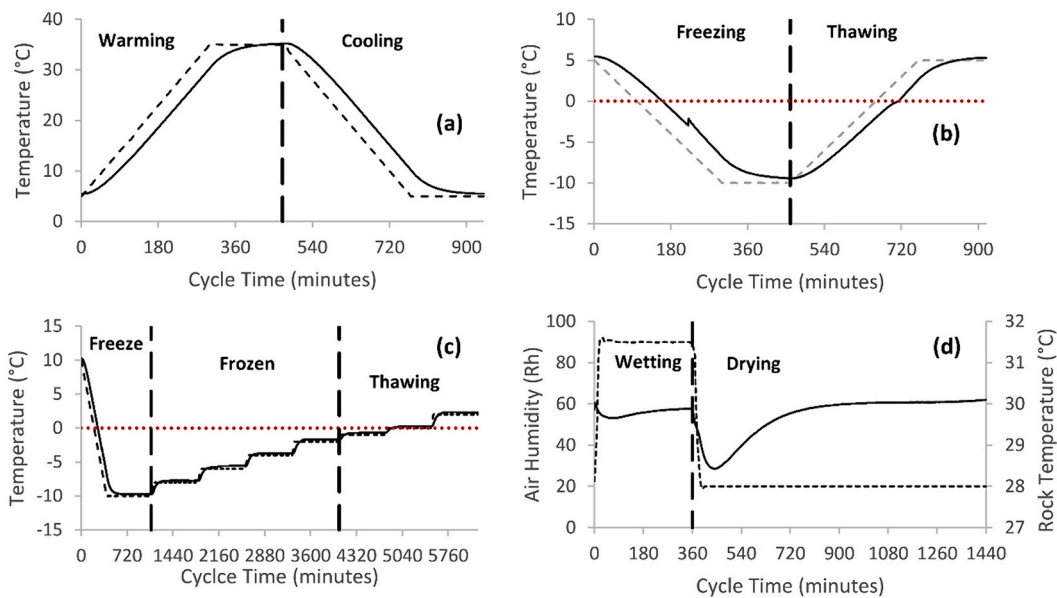
Fig. 1. (a) one W/C temperature cycle, (b) one F/T temperature cycle and (c) one LF temperature cycle showing air temperature in the climate chamber (dashed black line) and rock temperature (solid black line). 0 °C is shown by the red dashed line. (d) W/D cycle conditions with chamber air humidity (dashed black line) and rock temperature (solid black line).

Table 2
Models and accuracies of instruments used in experiments.

| Instrument	Measurement interval	Accuracy	Position	Depth	Additional information
Acoustic Emissions (AE) sensor	Constant (10 K samples/s).	35–65 kHz frequency range, ± 1.5 dB directionality	Top, centre of samples	Surface	Physical Acoustics 60Khz, Micro SHM logger, cable (5 m).
Temperature gauge	1 min	Resolution 0.01 °C, accuracy 0.03 °C.	Front side, centre of samples and near for air °C.	5 cm	Greisinger GTF 401 1/10DIN temperature sensors
Climate chamber	1 min	$< \pm 0.3$ °C, $< \pm 3\%$Rh stability	Samples inside.	N/A	Kambič KK-340 CHLT

to 35 °C (at a maximum warming/cooling rate of 6 °C/h) where used to simulate the weathering effect of samples in a temperature range potentially experienced by alpine rocks in the summer season. These Warming/Cooling cycles (referred to as W/C cycles from herein) shown in Fig. 1a were repeated 9 times.

Freeze/Thaw temperature cycles (920 min length) fluctuating between 5 °C to −10 °C (maximum cooling/warming rate of 3 °C/h) where used to check the weathering effect of samples in a temperature range potentially experienced by alpine rocks in the winter season. These Freeze/Thaw cycles (referred to as F/T cycles from herein) shown in Fig. 1b were repeated 9 times.

A longer freezing cycle of c. 4 days was used to simulate a freezing cycle seen during a longer period of cool temperatures in the Alps. The initial cooling rate of shorter 3 °C/h was used with a gradual stepped thawing process to decrease the thermal stress during thawing. This type of cycle was also used by Mayer et al. (2023) which enables comparability with their investigation. This longer freezing cycle (referred to as LF cycles from herein) is shown in Fig. 1c. was performed only once with samples at c.0 %, 50 % and 100 % rock moisture saturation.

For the W/C, F/T and LF temperature cycles' samples were wrapped in clingfilm to ensure constant moisture content and no wet/dry weathering effects. Temperature and air humidity were controlled with a Kambič KK-340 CHLT climate chamber with samples placed on a shelf, isolated by high density foam on which the samples were placed. For all experiments a temperature gauge was used in the centre of the blocks to asses rock temperature and a 4th gauge measuring the air temperature. Each sample also had an Acoustic Emissions (AE) sensor (Table 2) installed on the top centre of the samples to monitor AE hits caused by cracking events.

A final Wet/Dry experiment was conducted using three rock cubes. For this experiment the samples had no clingfilm with 4 sides of the sample open to climatic changes (see Fig. 2). A constant air temperature of 30 °C was maintained inside the climate chamber, to negate the effects of thermal stress seen in the temperature cycles and isolate the weathering effect of the wetting/drying process. As shown in Fig. 1d the cycles begin with a 6 h wetting phase where the samples sit in 15 cm² tray with 300 ml de-ionized water and the air humidity is adjusted to 90 %. For the following 18 h drying phase the wetting trays are removed
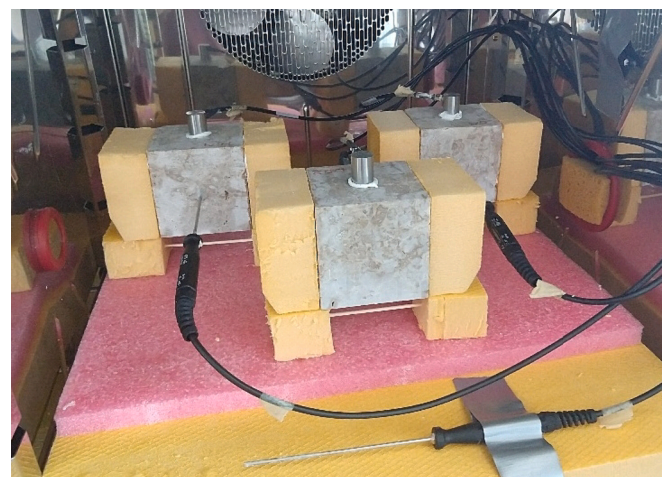
Fig. 2. Photo of experiment setup (drying of wet/dry cycles).

and the samples are raised to ensure 4 side ventilation and the air humidity was brought down to 20 %. Evaporative cooling causes a slight temperature fluctuation of 1.5 K (Fig. 1d).

2.3. Acoustic emissions

In order to monitor cracking one PK61 AE sensor (frequency 35–65 kHz) from Physical Acoustics was installed at the top of each sample using acryl. A Physical Acoustics Micro SHM node was used to record the AE data. Processing of the AE data was done using AEWin software, with a threshold of 30 dB to ensure no electrical background noise from the sensors. So that background noise from the climate chamber was separated from actual microcracking events, a filter based on pencil lead break tests (Sause, 2011) of the sample blocks was used.

Throughout the experiment data acquisition was continuous with AE hits, Time of AE hit, Peak Amplitude (dB), Counts, Rise Time (ms), Duration (ms), Average Frequency (kHz), Absolute energy (aJ or atto-Joules), Peak Frequency (kHz) being among the AE signal parameters collected (see Fig. 3a). From these features, parameter based, SiGMA and waveform based analysis can be performed. For this study we chose to use parameter based analysis because of the decreased need for computing power compared to waveform analysis. Also, SiGMA analysis (Ohno and Ohtsu, 2010) needs at least 6 sensors per sample, so it is not possible with the current set up and the distances involved in our small samples should make the effect of signal attenuation negligible.

In order to classify the mode of cracking the empirical relation of Average Frequency (1) and RA value (2) (Ohno and Ohtsu, 2010) is often used in concrete testing and increasingly used with rock samples. They were calculated as below:

$$\text{Average frequency (kHz)} = \text{AE counts/duration time (ms)} \quad (1)$$

$$\text{RA value (ms/V)} = \text{rise time (ms)/maximum amplitude (V)} \quad (2)$$

As shown in Fig. 3.b based on Japanese construction code JCMS-IIIB5706 (2003) these two parameters can be classified as Tensional mode (higher AF, lower RA) and Mixed/Shear mode (lower AF, higher RA). The convention used in JCMS-IIIB5706 (2003) suggests a separating line of 0.1 kHz ms/V for the two cracking modes, however a defined criterion for this separation line does not exist (Ohno and Ohtsu, 2010) and the mechanical properties of Wetterstein limestone are quite

different to that of concrete.

Many studies are now looking at micro cracking mode in rock samples (Dong et al., 2022; Li et al., 2022; Wang et al., 2021; Zhao et al., 2023; Du et al., 2020). The problem with all of these studies is that the line of separation for the Tensile and Mixed/Shear cracking mode is difficult to define and varies greatly between different materials. There are a multitude of methods tried by authors to solve this problem including Kernel Density Estimation (Li et al., 2022), k-means (Wang et al., 2021) and mechanical testing (Du et al., 2020; Li et al., 2022). The most reliable method appears to be using destructive mechanical tests: Direct Tensile test, brazillian and shear tests to calibrate to the specific lithology the optimal separation line (Deresse et al., 2023). Unfortunately, such mechanical tests were not in the scope of this project. So, for this study the data was first normalized (min-max) and the dividing line for Tensile and Mixed/Shear Mode cracking was given as a 1:1 slope of the normalized data (as in Dong et al., 2022). This will create some error/misclassification of cracking mode, but will still provide a solid impression of cracking mode changes.

3. Results

3.1. Warming/cooling cycles

The cycle is divided into a warming phase from 5 °C to 35 °C and a cooling phase from 35 °C to 5 °C (Fig. 4). The greatest temperature gradient between the air around the surfaces of the stone and the interior of the stone is reached approximately in the middle of the two halves, i. e. at approx. 245 min and 715 min. Fig. 4 shows the cumulated sum of all 9 cycles.

Total cumulative AE hits range from c.600 to c.1700, with no apparent relation to moisture content. The cooling phase sees a higher overall number of AE Hits, occurring more or less continuously over the half-cycle, than for the warming phase. We attribute this to the higher stresses generated by contraction (cooling) than by pressure (warming). During the warming phase, AE hits are concentrated in the first c.90 min of the cycle. This could be caused by an increased hydrostatic pressure caused by simultaneous expanding of rock moisture volume and contraction of pore space from the expansion of the rock mass on warming. This could also explain that the more saturated samples have greater hits at this point and even greater relative hit energy. This effect
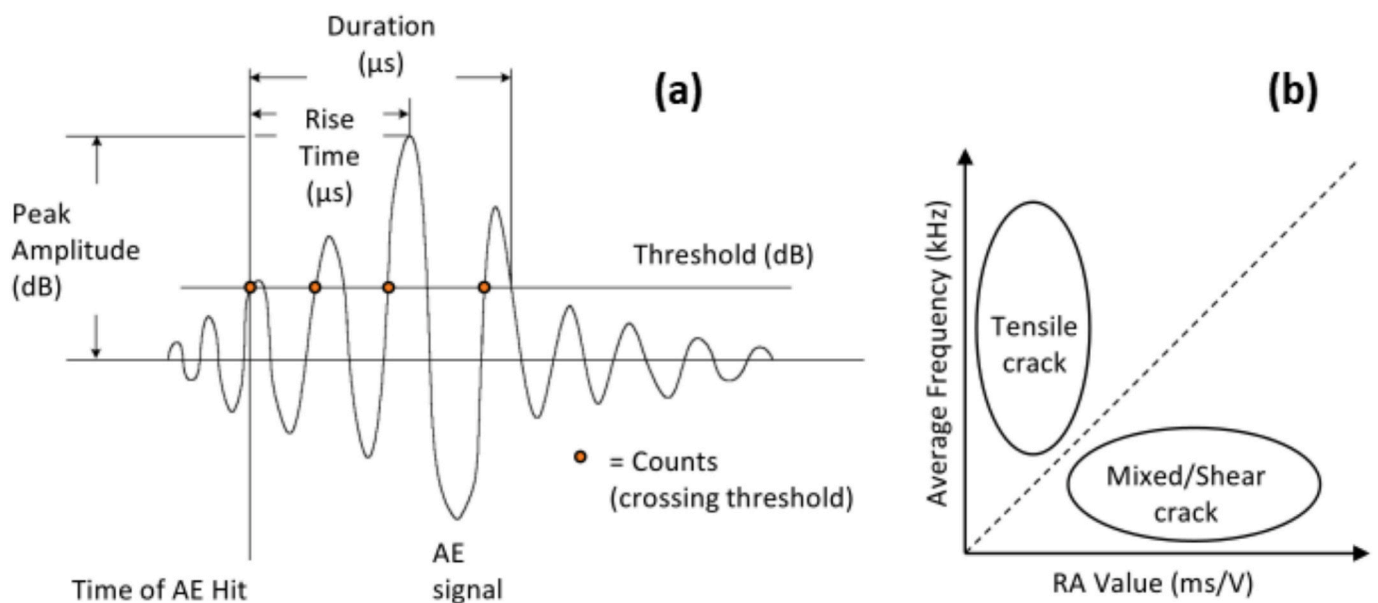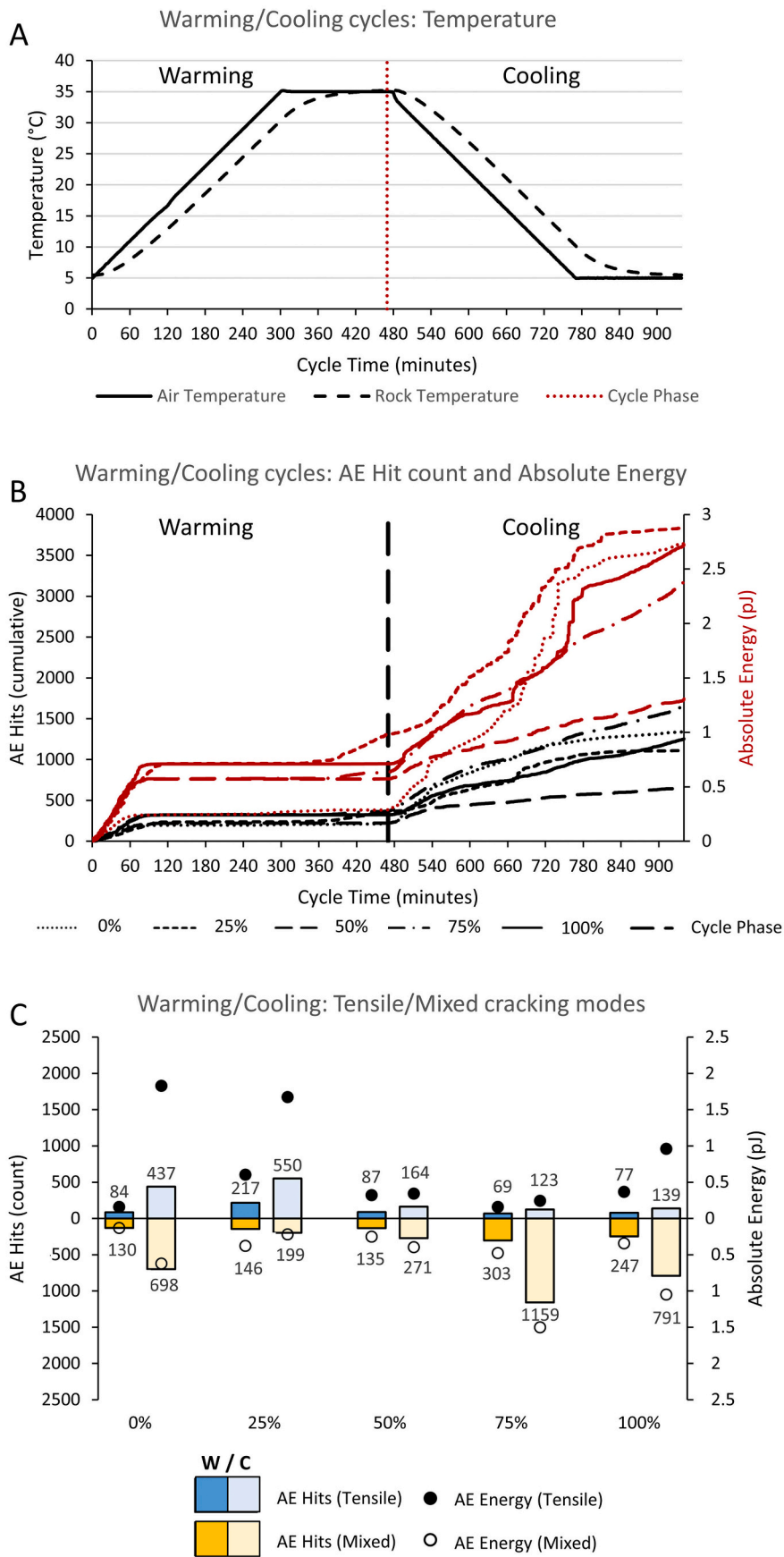

Fig. 3. a) schematic of waveform parameters of acoustic waves and b) RA-AF plot used to discriminate between tensional and shear fracture modes (modified from Ohno and Ohtsu (2010).

Fig. 4. Results of W/C cycles shown in (A) Warming/ Cooling cycle (repeated 9 times during experiment) rock and air temperature, (B) cumulative sum of AE hit count and Absolute Energy shown for all 9 cycles at different rock moisture % saturation and (C) cycle phase split of cracking mode (Tensile and Mixed mode) and sum of energy at different rock moisture % saturation.

is however short lived compared to the AE events in the cooling phase which occur more or less continuously over the half-cycle. The curves for of 0 %, 25 % and 100 % saturation show a clearly pronounced maximum near the middle of the cooling phase, coincident with the period of the highest temperature gradient.

In Fig. 4 parameter analysis of the AE data shows a greater percentage of tensile mode cracking under less saturation (0 % & 25 %) and consequent higher energy release. This could be due to the higher ductility of the fracture surfaces in samples with greater free water content and possibly in a small part to attenuation of AE signal when samples have higher saturation.

3.2. Freezing/thawing cycles

The cycle consists of a cooling phase from 5 °C to −10 °C and a thawing phase from −10 °C to 5 °C (Fig. 5). Again, highest temperature gradients within the stones are found in the middle of the two half-cycles. In the freezing phase, an exotherm can be seen at approx. 230 min when a significant amount of pore water freezes (temperature curve taken from average of 100 % saturated experiment). Fig. 5 shows the cumulated sum of all 9 cycles.

Total cumulative AE hits range from c.1700 to c.3800 (Fig. 5). Rather than affecting the cumulative AE hit count, rock moisture is seen to strongly effect where these cracking events occur in the cycle and the cumulative energy of them. For the 0 % samples, the AE hit count follows the temperature gradient seen during the cycles, with a greater rate of AE hits during increased thermal gradient in the rock in both the Freezing and Thawing phase. However, with increasing rock moisture saturation there is a trend for cracking events occurring later in the freezing phase. This is probably due to greater volumetric water content needing longer to freeze. It is also noted that the rate of AE Hits in the higher saturation (100 %) is much greater through the late freezing and early thawing stages. During the Thawing phase higher saturation (75 % & 100 %) shows AE hits almost entirely stopping in the period after c.660 min, while with less saturation (25 % & 50 %) AE hits continue at a reduced count after this point. We assume that refreezing events are more frequent at lower saturation because there is still available pore space for the water to move. At 100 % saturation, freezing causes cracking events but there is no pore space left for refreezing events during thawing.

Absolute Energy released is by far the highest at 0 % saturation (note separate y axis in Fig. 5). Where this peak in energy occurs is evidence that the sample is not completely "dry" because, as discussed in materials and methods section, although all the free water has been removed in the drying process there will still be some interstitial pore water left in the rock samples. The volumetric expansion of this is most likely to cause higher energy tensile cracking. As with the warming/cooling cycles, we assign the disparity in energy release to a more brittle deformation of the dry stone and to a lower attenuation of the acoustic signal. Released Energy curves for more saturated experiment runs also show this defined increase in cracking energy, correlating with the isotherm in the temperature curve at c.240 min seen in Fig. 5. Notably, for the higher rock moisture saturation experiment runs this period of increased AE activity starts later but has a longer duration than the lower saturation runs.

3.3. Long freezing cycle

The long freezing cycle has a longer duration of the minimum temperature (−10 °C) and a slow, stepwise temperature increase in the frozen and thawing phases (Fig. 6). Three Wettersteinkalk samples were used with different rock moisture saturation (0 %, 50 % and 100 %).

Total cumulative AE hit count range from c. 650 to 3000 depending on rock moisture content. The 0 % sample shows the lowest AE count in the long freezing cycle (Fig. 6). Almost all of these AE hits are in the Freezing phase, with the greatest intensity and energy from c.300 to 400 min probably due to thermal contraction. As in the above mentioned

experiments, the released energy is much higher than in the more saturated (50 % & 100 %) samples, which is probably again due to AE signal attenuation by pore water.

During the freezing stage the 100 % saturation sample shows the most AE hits, closely followed by the 50 % sample (2359 to 2002 AE hits respectively). Notably the timing and longevity of increased AE hit count is in line with delayed freezing of samples due to increased rock moisture content. The 0 % samples AE hit rate increase greatly from c.300 to 400 min. For the remainder of the freezing cycle it decreases to a fairly constant rate, in line with a steady state temperature of rock sample and air. With increased rock moisture saturation, the 50 % sample shows and increase in AE hit rate from c.400 to 500 min, while the 100 % sample shows a longer period from c.500 to 950 min. Both the higher saturation samples show evidence of probable refreezing with one or more periods of decreased AE activity followed by a sharp increased. This can be seen in the 50 % sample from c.440 to 460 min and in the 100 % sample in 2 stages at c.540 to 580 and c.710 to 760 min.

Almost no AE hits occur during the long frozen stage for 0 % and 100 %, however for 50 % some do during the increase in temperature from −10 °C to −8 °C. We assume that in this stone there is still pore space available for moisture movement to crack tips, while in the 100 % stone the entire pore space is already occupied and there is no free water in the 0 % stone. Both 50 % and 100 % samples show an increase in AE activity in the thawing phase, after the stones have returned to ≥0 °C. This may be due to meltwater spreading through the cracks causing hydration of fracture walls in newly formed porosity.

Unlike in the shorter freeze/thaw cycles discussed earlier, the cracking is predominantly tensile mode in the freezing phase of the 50 % and 100 % samples (Fig. 6); also the cracking mode in the frozen stage is almost entirely tensile mode.

3.4. Wetting/drying cycles

The cycles consist of a wetting phase at 90 % air humidity with the samples each sat in 300 ml of water, and a drying phase at 20 % air humidity, not sat in water (cycle repeated 7 times). Air temperature was kept constant, but slight cooling (1.5 K) occurred in the beginning of the drying phase due to evaporation (Fig. 7).

Most AE hits occur in the wetting phase, with most of those being in the initial 40 min of the cycle (Fig. 7) during which time the humidity changes from 20 % to 90 % and capillary rise begins to wet the stone. The cracking events are probably due to water penetrating into small cracks and exerting electrostatic pressure. Cracking mode in this phase is predominantly tensile (Fig. 7). After the first 60 min of the drying phase there is a pronounced peak of AE events, when the humidity gradient reverses and evaporation sets in. Further cracking events occur more or less continuously during the drying phase; one event at c.1200 min caused a slightly higher energy release, maybe due to contraction upon drying. The cracking mode in this phase is partly tensile and partly mixed with a lower tensile energy release than during wetting.

3.5. Comparison of effective porosity increase in different cycles

The W/C cycles have the greatest thermal stress induced by the cycle with 6 °C/h temperature gradient, twice that of the F/T cycles (3 °C/h). The gained Effective Porosity of the W/C & F/T is however very similar (see Table 3). This would suggest that the increased weathering effect of the moisture present in the F/T cycle causes nearly the same weathering effect as the thermal stress from a 3 °C/h temperature increase above freezing.

Comparison between the different rock moisture content effects on effective porosity increase is not possible as only the start and end effective porosities are known between the samples. In future work it would be good to measure effective porosity change after each moisture experiment. However, this should be done with separate samples for each moisture content as repeated wetting and drying of samples would
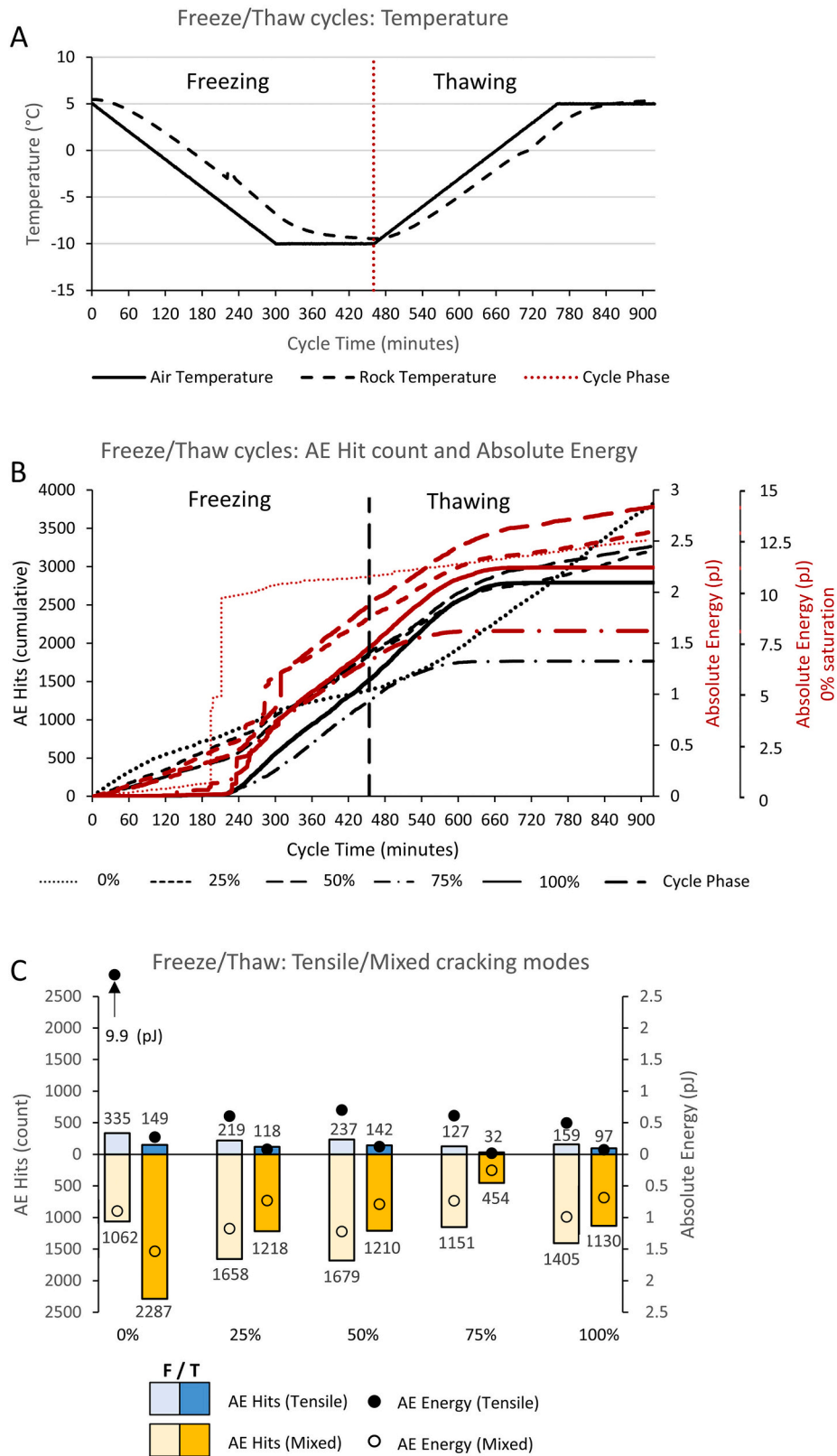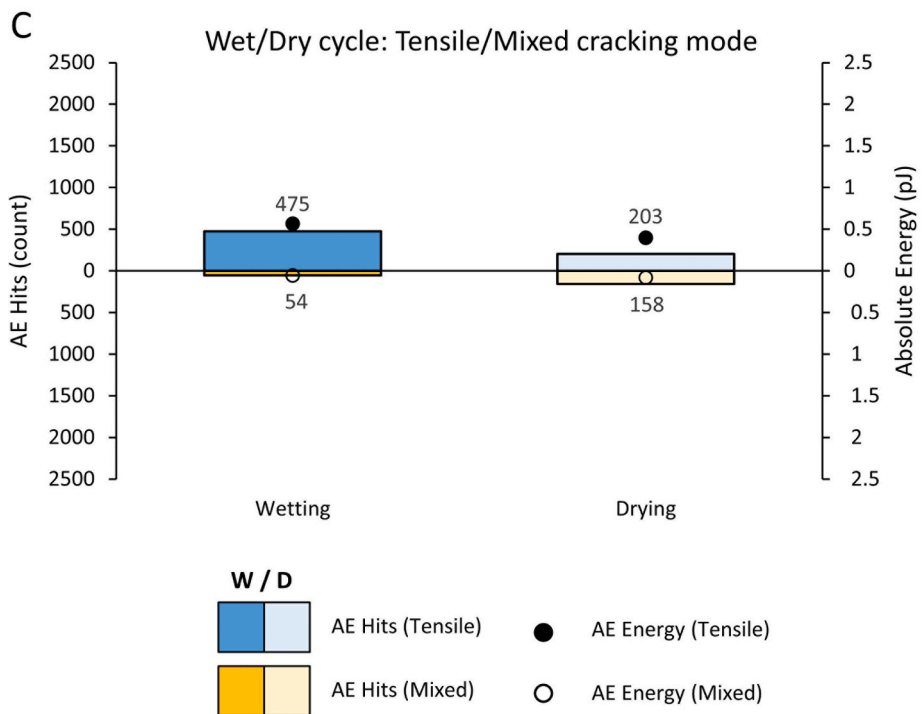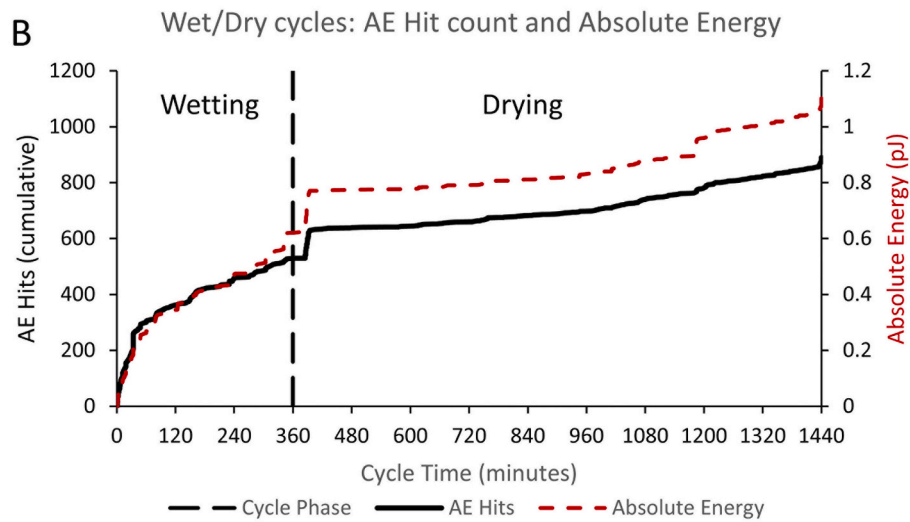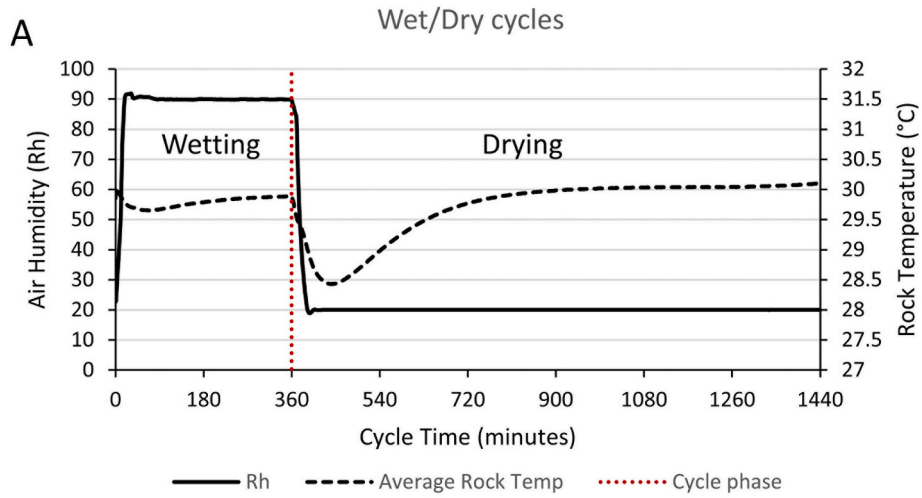
Fig. 5. Results of F/T cycles shown in (A) Freeze/ Thaw cycle (repeated 9 times during experiment) rock and air temperature, (B) cumulative sum of AE hit count and Absolute Energy shown for all 9 cycles at different rock moisture % saturation and (C) cycle phase split of cracking mode (Tensile and Mixed mode) and sum of energy at different rock moisture % saturation.
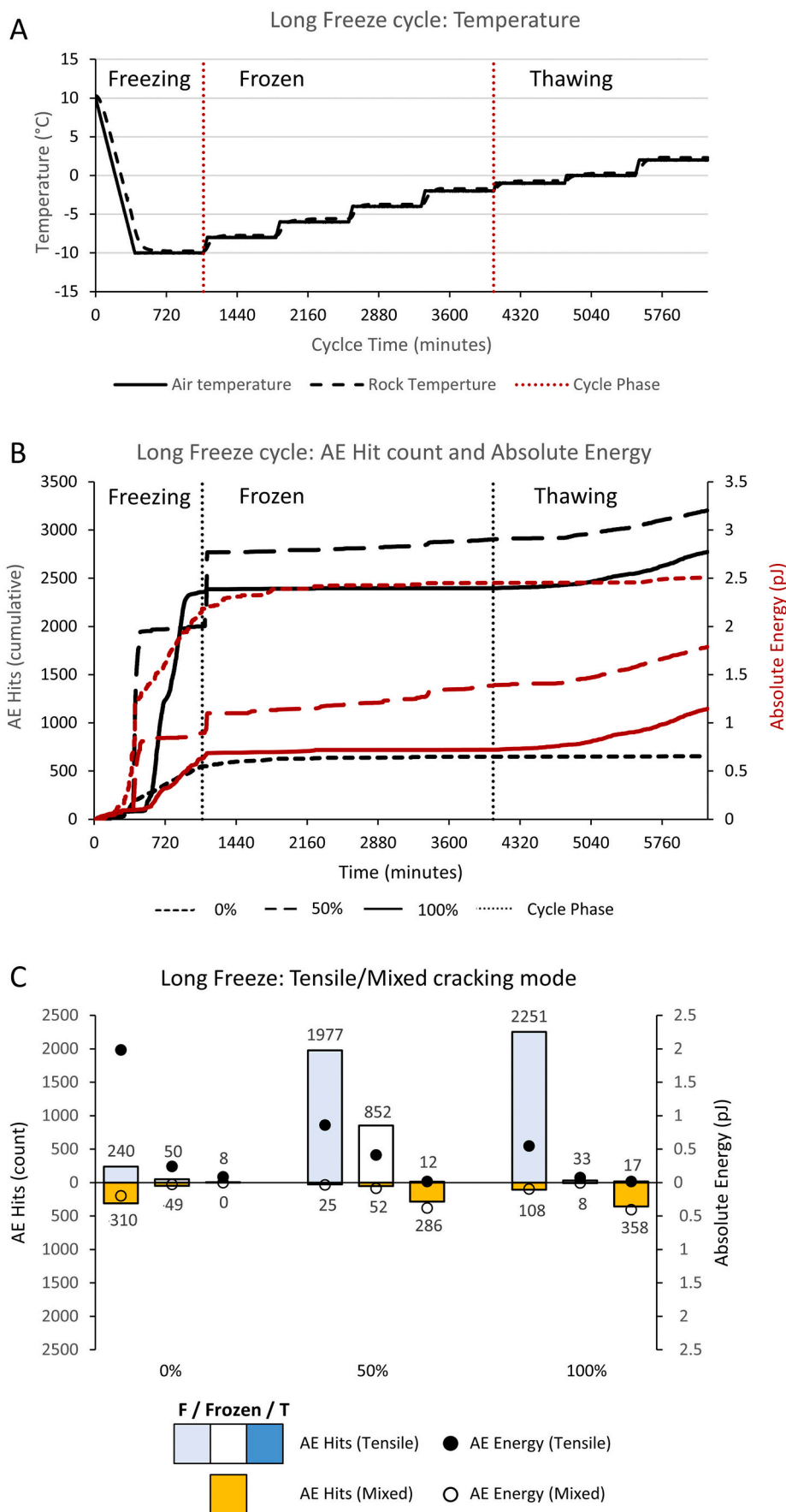
Fig. 6. Results of Long Freezing cycle shown in (A) Long Freezing cycle rock and air temperature, (B) cumulative sum of AE hit count and Absolute Energy shown at different rock moisture % saturation and (C) cycle phase split of cracking mode (Tensile and Mixed mode) and sum of energy at different rock moisture % saturation.

(caption on next page)

cause further weathering that would need to be quantified.

For the LF cycles the results show that the 0 % sample has half the effective porosity gain of the more saturated 50 % and 100 % samples. Interestingly the weathering effect of the 50 % and 100 % samples is very similar. This is seen in both the weight difference and relative AE hit count.

The W/D cycles sample weight difference corresponds to the difference in AE Hits and Energy seen in tests with W/D1 producing by far the lowest count. Also, capillary uprise tests showed the W/D2 also was able to gain the most water. In each 6 h wetting period 71.3 % of total effective porosity was filled, compared to 63.3 % in W/D3 and 57.8 % in W/D1. This suggests there is an exponential relationship between the % of effective porosity that can be hydrated and chemically weathered by rock moisture and it's weathering effect. This may have to do with the extra hydrostatic pressure forcing the rock moisture into areas in the fracture network where wetting of less % porosity volume would not migrate to.

3.6. Comparison of AE hit count and energy released over 4 days

In order to compare relative weathering effect on the rock samples of the different weathering cycles a period of c.4 days duration was chosen. This allowed for 6 complete W/D and F/T cycles, 4 W/D cycles and up to 5760 min of the LF cycle.

The results of this (Fig. 8) show that the LF cycle has by far the greatest weathering effect of the weathering cycles in more saturated samples, with the AE hit count being >3× that of equivalent saturation during the other weathering cycles. This would suggest that the shorter duration of the F/T cycles, compared to the LF cycles, meant there was insufficient freezing time for enough of the available rock moisture in the samples to change phase to ice. Thus, the increased weathering effect possible from the volumetric expansion of greater water volume did not occur. Further to this point, the drier 0 % samples for the LF and F/T cycles can be seen to have comparable AE hit count and Absolute Energy release.

Comparing the effects of F/T and W/C cycles the F/T has >2× AE hit count for equivalent rock moisture content. Aside from 0 % F/T, the energy dissipated is however comparable. This AE hit energy disparity is probably due to the increase in AE hits being largely mixed mode cracking (see Figs. 4 and 5) in F/T, while the greater thermal stress seen in the W/C cycle appears to make the rock sample more prone to higher energy tensile mode cracking.

While samples in all the other weathering cycles were sealed from the atmosphere with clingfilm to prevent the effects of wetting/drying, the AE count and energy released show that the effect of the W/D cycles on rock strength should not be discounted. In fact, it would add measurable amounts of extra weathering to all the other weathering cycles tested.

4. Discussion

4.1. Limitations of study

There are some important factors affecting rock weathering which this study does not take into account. The physical breakup of rocks is often accelerated by chemical weathering, particularly in limestones with high moisture content. This is potentially increased with increased subcritical cracking due to the greater surface area of available rock. Levenson and Emmanuel (2013) suggested polished rock surfaces may in fact accelerate rock surface dissolution in locations where the polished surface intersects a pore. This could affect our results application to field settings as all the samples used had smooth sawn surfaces, which are not at all comparable to the rough natural rock surfaces seen in the field.

Where the samples were collected could also have an effect on the results. A quarried rock face will have a different stress history to that of a natural rock slope, particularly due to extraction techniques (Voigtländer, 2020). Therefore, there is the possibility that this could affect the results, however samples collected at rockwalls directly will have biases of their own. The advantage of taking the samples from a quarry environment is that we were able to take samples from the same area and block, so ensuring as similar a stress history as possible and removing experimental biases from the effect of this variable.

Though the effects of thermal cycling and freezing due to air temperature changes are covered in this study, the effect of thermal stress due to solar insolation which would create an even greater thermal
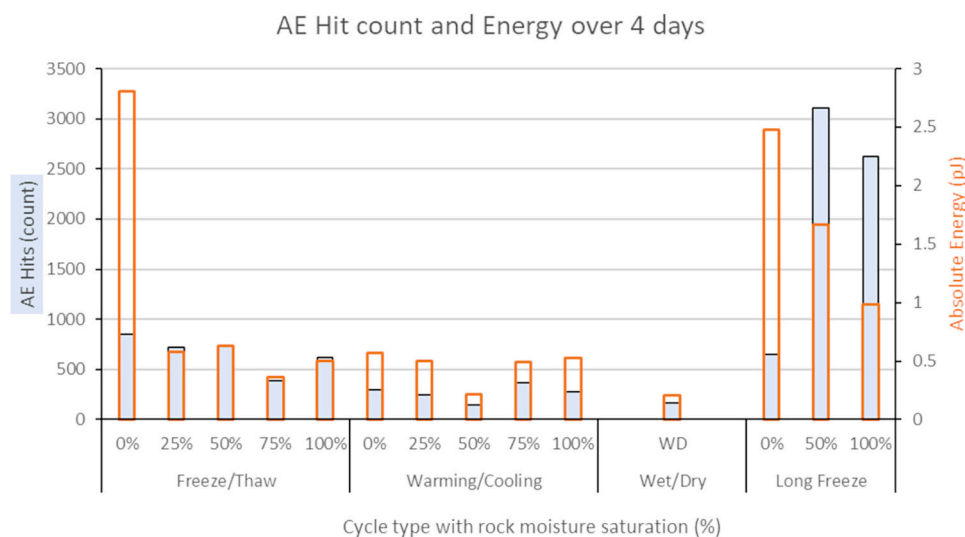
Fig. 8. Weathering effect of different weathering cycles and rock moisture % compared over c.4 day period (F/T: 5520 min, W/C: 5640 min. (6 cycles), WD (4 cycles) & LF 5760 min).

gradient is not. In a field study using AE sensors Eppes et al. (2016) found solar insolation causes sufficient thermal stresses to initiate subcritical cracking. Another assumption is that the distribution of moisture through the sample blocks is assumed to be even throughout the experiment. There is however a possibility of moisture movement at all saturations during the experimental climatic cycles and to water being expelled from the porosity during temperature cycles.

Furthermore, there is a non-linearity of rock degradation during freeze/thaw cycles (Martínez-Martínez et al., 2013). Over time micro cracks coalesce to form macrocracks and eventually leading to major failure of the rock sample. Martínez-Martínez et al. (2013) found that for lower porosity limestones (<10 %), like the samples in our study, development of microcracks was noticed, but complete failure of the rock did not occur within 96 freeze/thaw cycles. Therefore, it would be of interesting in future experiments with Wetterstein Limestone to increase the number of cycles to see when macro-crack formation begins and so major weakening of an alpine rockwall. Finally, only a limited number of rock samples were used for each test run. Therefore, we cannot discount that the randomness of individual rock samples has impacted the experimental results.

4.2. Rock mechanics and AE signal attenuation with rock moisture

Throughout the experiments it has been observed that the amount of rock moisture and available porosity affects when and how much cracking activity occurs. While the amount of cracking events in W/C cycles is not altered by rock moisture content, there is a significant effect on the timing in F/T cycles. With increased rock moisture there is an increase in AE hit "quiet periods" and greater energy release per cracking event in drier rocks. The reasons for this are thought to be due to AE signal attenuation caused by rock mechanic changes.

The phenomenon of AE signal energy dissipation with increased rock moisture has been observed in many studies (Ranjith et al., 2008; Lin et al., 2019; Guo et al., 2018; Dong et al., 2022) and signal frequency is also seen to be reduced (Liu et al., 2019 & Zhu et al., 2020). H. Li et al. (2021) went further to suggest that this phenomenon in saturated sandstones can be attributed to more intergranular fractures occurring with higher rock moisture, leading to peak AE hit energy being half that of drier samples. This weakening effect of rock moisture on rock fracture properties, causes a reduction in the instantaneous elastic energy release during the large-scale rupture of rocks (Zhou et al., 2018). In addition to this, Zhu et al. (2020) suggest a friction reduction owing to lubrication of joints also creates a reduction in fracture energy. These changes in rock mechanics could explain the lower rate of AEs from cracking in increasingly saturated samples and the increased likelihood of high energy events in the more brittle behavior of drier rocks.

Further to this Kodama et al. (2013) found water saturated blocks had an inverse strength relationship to temperature, becoming stronger as they freeze. They suggested that part of this strength change is due to a reduction in stress concentration within the interstitial spaces and cracks in rocks. When these saturated blocks then thaw the strength can decrease by as much as 50 %, causing destabilisation at degrading permafrost boundaries (Krautblatter et al., 2013). In the case of Wettersteinkalk specifically, Eppinger et al. (2018) found that the Young's Modulus decreased by 20 % from frozen to unfrozen saturated samples and even more at 27 % frozen to thawed dry samples. This change of

mechanical properties with rock moisture is particularly visible in our Freeze/Thaw cycles, with decreasing AE cracking events at the beginning of freezing and end of thawing correlating with increased rock moisture.

4.3. Time needed for rock moisture to change state

We found that duration of temperature cycles is an important factor in rock weathering, particularly affecting freezing cycles. During the shorter F/T and W/C cycles, there is little effect on the overall number of cracking events with changes in rock moisture. The only exception to this is at the first c.90 min of the warming cycle where the number of cracking events and especially dissipated energy is far greater than the c.0 % drier samples. We propose that this is due to thermal expansion causing crack closure and creating a hydrostatic pressure in the crack tips of more saturated samples.

During the cooling period of the W/C cycles, there is a much greater energy released per AE hit than in the F/T cycles (apart from the exception of the 0 % F/T cycle). We proposed that this is because of the increase in thermal stress due to double the rate of climatic thermal gradient. The F/T cycles do produce a much greater AE hit count, though the overall count does not appear to be affected by rock moisture. However, with the increased freezing time of the LF cycle the change with the presence of rock moisture becomes apparent, with over double the increase in effective porosity and over 4× the AE count. Changes in effective porosity meanwhile, show at least double the increase in effective porosity between dry and more saturated samples (Table 3). We propose that the difference in these two weathering markers (AE hit count and effective porosity increase) is due to that fact that not all weakening of the rock through cracking will cause an increase in permeability. For example, any vuggy porosity or interstitial water that is not connected to the permeable porosity, will not cause an increase in effective porosity even if there is considerable subcritical cracking (and so weakening of the rock mass) in this area. Furthermore, while shear deformation can cause permeability increase through shear dilation, it can also cause decreases in permeability due to shear compaction and clogging of fracture from gouge formation (Li et al., 2023). For this reason, the authors argue AE hit count is a more complete determiner than change in effective porosity.

Finally, a further effect of the increased freezing time and ice formation in the LF cycles is seen during the thawing stage of the cycles. Here it is the more saturated samples that show more cracking activity due to unloading effect of melting ice and occasional re-freezing events. The 0 % sample shows nearly no AE hits during the thawing period, which is at odds with the findings of the shorter F/T cycles. This is probably due to the much more gradual, stepped warming of the LF cycle putting less thermal stress on the samples.

4.4. Cracking mode as seen in other studies

Changing cracking mode in weathering cycles can be used to determine the likely mechanism of sub-critical crack propagation. In the long-term freeze/thaw experiments of Maji and Murton (2021) they suggest that at lower temperatures (−15 °C) Tensile mode cracking is dominant suggesting volumetric expansion as the cause. Meanwhile, at higher temperatures (though still sub-freezing at −10 °C to −5 °C) were

Table 3

Shows the effective porosity gained after all cycles completed. Calculated by oven dry (60 °C) and saturated (submersion) weight difference before and after cycles.

Cycles	Warming/cooling (W/C) (×9 cycles, 920 min/cycle) 0 %, 25 %, 50 %, 75 %, 100 % moisture sat.			Freeze/thaw (F/T) (×9 cycles, 940 min/cycle) 0 %, 25 %, 50 %, 75 %, 100 % moisture sat.			Long freeze (LF) (×1 cycle, 6224 min)			Wet/dry (W/D) (×7 cycles, 1440 min/ cycle)		
Sample	W/C1	W/C2	W/C3	F/T1	F/T2	F/T3	(LF1) 0 %	(LF2) 50 %	(LF3) 100 %	W/D1	W/D2	W/D3
Effective Porosity (% vol.) increase	0.175	0.305	0.275	0.325	0.205	0.305	0.105	0.21	0.225	0.05	0.125	0.115

associated with more shearing cracking.

In the freezing phase of our LF experiments the 0 % sample shows a fairly even split of Tensile and Mixed mode cracking, while the more saturated samples show an almost purely Tensile mode cracking (in line with Maji and Murton's (2021) observations). We propose an initial period of crack propagation caused by hydrostatic pressure build in the crack tips in line with ice formation (Sass, 2004). Then, when ice volume reaches a critical mass later in the process of ice segregation, volumetric expansion takes over as the dominant process. That is not to say that the processes happen in isolation, rather they interplay.

We propose that the thermal stress caused by the temperature change from $-10\,°C$ to $-8\,°C$ cause an increase of confining pressure enough to melt some of the ice, which is then transported by cryosuction and re-frozen (Gerber et al., 2022), causing a period of increased cracking activity. There is only a small peak in the 100 % sample and a much larger peak in the 50 % sample. We propose this is due to the fact of the 50 % sample being weaker due to less pressure being supported by ice, but still with available supercooled water that can cause increased pressure through volumetric expansion at fracture tips.

During Thawing phase there is a switch to Mixed mode dominated cracking as seen in Maji and Murton (2021). We agree with their suggestion that this could be due to a partial melting of ice providing an increased volume to the thin film of pellicular water (Xu et al., 2022), creating a reduction in friction and destabilising the rock/ice boundary (Krautblatter et al., 2013). This could also help explain the dominance of Mixed mode cracking in the shorter Freeze/Thaw cycles as there is still a majority of water and not ice, so the rock mechanics are inclined to Mixed/shear mode cracking. Furthermore, Shear stresses can cause the removal of segments of fracture surface progressively smoothing the surface (Meng et al., 2016), lowering the fracture toughness and causing debris which could increase weathering through "grain wedging" (Musso Piantelli et al., 2020) during freeze/thaw cycles.

4.5. The importance of wetting and drying

The other experiments sought to exclude the effects of wetting and drying by being in a closed system. In real world (alpine) settings, this is rarely the case with moisture movement coming from deeper in the rock where the rock is generally moist (c.80 % at 20 cm depth; Sass, 2005) and wetting and drying processes occurring near the rockwall surface.

Wetting/Drying cycles were shown in our experiments to have a measurable effect, comparable in effect to AE hit count seen in the W/C cycles of the same duration (see Fig. 8). In earlier studies Hudec and Sitar (1975); Nepper-Christensen (1965, p. 555) found the average expansion upon wetting was comparable to thermal expansion seen in the field. The results from our experiment show wetting to have the greater weathering effect of the 2 phases, with most cracking occurring within the first 60 min (see Fig. 7). Yatsu (1988) suggested cracking events occurred during the expansional wetting phase only. Our experimental results suggest this is not the case, with AE hits also occurring during the drying phase with a greater mixed/shear cracking mode proportion. With increasing wetting/drying cycles this subcritical cracking leads to a degradation of mechanical properties in rocks, dependent on lithology (Zhang et al., 2021).

Effective Porosity changes (one measure of cracking activity) after W/D cycles were significantly lower compared to the other weathering cycles with an apparent relation to starting effective porosity (see Table 1 & 3). In experiments by Meng et al. (2019) they put agrillaceous limestone samples through 72 h cycles of wetting and drying at room temperature. They found a significant increase in effective porosity after 6 cycles. As our experiment only had 7 diurnal cycles, we would suggest future work with Wettersteinkalk should consider longer cycle durations to see if a similar effect occurs. Part of this effective porosity increase may also be due to dissolution, the effects of which increase in warmer climates (Hall, 2013; Eppes et al., 2020) and so most likely effecting our W/D cycles conducted at $30\,°C$.

Then comes the question of how much of an extra effect wetting and drying would have on the weathering processes studied under open rather than sealed conditions. As a process it is thought to play a synergistic role with other weathering processes (Hall, 2013). For the W/C cycles there would probably be a component of wetting/drying in all stages of the of the cycle, meanwhile the F/T and LF cycles would likely see wetting and drying in the Thawing phase and those above freezing. Pissart and Lautridou (1984) and Moss et al. (1981) both see W/D as synergistic with F/T weathering with the combination even leading to an increase in rock breakdown, though frost weathering was found to have 3–4 times greater weathering effect than pure hydration (Moss et al., 1981). This ratio of W/D to F/T weathering effect is also seen in our experiments (see Fig. 8).

From field studies in Alaska and Antarctica by Hall (1991, 1993) it was argued that even in the subsurface wetting and drying is taking place, due to rock moisture movement. This would result in potential synergetic effects of wetting and drying on other processes going undetected. Moisture movement itself can cause limestone weathering rates to increase in higher saturations dominated by capillary transport, due to micron-scale grain detachment (Emmanuel and Levenson, 2014). At lower saturations transport modes of pore water differ, becoming increasingly hygroscopic and below 20 % humidity vapour diffusion is the main mode of moisture transport in pores (Stück et al., 2013; Kießl, 1983). It is suggested by Eppes et al. (2020) that an increase in water vapour pressure itself can cause the propagation of subcritical cracking at crack tips. We propose that this explains the greater number of AE events seen in the LF cycles of 50 % saturation, due to components of moisture transport including vapour diffusion, capillary condensation and causing the filling of bottlenecks (such as crack tips) with water. This means the rock moisture can still be at the most areas to propagate subcritical cracking at a similar level to fully saturated rocks.

4.6. Implications for rock weathering in alpine environments

A recurring theme is that not necessarily the more water the better. Just having rock moisture present can make a difference. Not much rock moisture is needed to make a difference. This has implications for the efficacy of weathering processes in alpine environments.

Our experiments showed that with sufficient time frost weathering potentially causes as much rock deterioration at 50 % effective saturation as at 100 % saturation. This means that less rock moisture may be needed for frost weathering action than previously thought. Even in shorter freezing cycles, where there is insufficient time for ice development in more saturated rockwalls, the presence and amount of rock moisture available affects the mechanical properties of the rock and where in temperature cycles the propagation of subcritical cracking occurs. Rode et al. (2016) and Sass (2005) showed that while moisture varies greatly throughout the year in the outer 5 cm of alpine limestone rockwalls the fluctuation is between c.60 % to 80 % pore water saturation, meaning the longer duration freeze/thaw cycles in these areas are prone to higher levels of frost weathering. Our research suggests that even at 50 % saturation, and probably even lower, there is a marked increase in relative weathering effect for such cycles.

The wetting and drying process has been shown to be an important contributor to rockmass deterioration and its effects should be included in any rockwall weathering model. It has particular implications to southern facing rockwalls which have large temperature and rock moisture fluctuations, creating the possibility for numerous cycles of wetting and drying and thereby weakening the near surface through physical cracking and chemical alteration. Additionally, the physical position in a larger rockwall has a bearing on rock weathering. Eppes and Keanini (2017) suggested that in near surface environments, the resulting increase in confining pressure caused by overlying rock mass may actually inhibit rather than increase subcritical cracking. Rockwall overburden of around 20 m is thought to be a "shut off" pressure for ice segregation (Krautblatter et al., 2013).

Finally, all samples were only of one lithology type and low porosity. This is commonly not the case in alpine rockwalls, with large heterogeneity in mechanical/chemical properties and porosity seen, even in the same lithology. This means many areas of the rockwall will behave differently to the weathering cycles presented in this study.

4.7. Effect of climate change on weathering regimes

The projected climatic changes in the alpine region to 2100 could be in the range of up to 0.5 °C per decade (Gobiet et al., 2014). The elevation of our ClimRock project areas in the field are in the range of 1300 to 2700 m. According to Gobiet et al. (2014) there would be on average c.4 °C increase in all seasons and altitudes, with up to 5 °C increase in the summer at higher altitudes. This is a significant change that will also impact precipitation and snow levels in an uneven distribution over different seasons and altitudes. During Winter precipitation is projected to increase 10 to 15 % (Gobiet et al., 2014) while less precipitation is expected in Summer. The intensity of precipitation events is expected to increase with Rajczak et al. (2013) suggesting the northern Alps could see as much as a 30 % increase in precipitation in future Autumns. Less precipitation, particularly at lower altitudes during summer, would probably see thermal stresses become the dominant preparatory weathering process. Based on laboratory results, this should not affect the overall weathering in this period due to this process apparently not being affected by rock moisture content. However, increasing precipitation intensity would increase the dominance of wetting and W/D cycles.

The work of Bajni et al. (2021) on the Aosta Valley showed a seasonality in both preparatory and triggering weathering indices for rockfall (F/T, W/D, Precipitation and thermal stress). Freeze-thaw cycles were shown to have by far the most connection to rockfall events in spring at 70 % as a lone index, while the water input from rainfall and snowmelt accounted for 49 % of rockfall events in autumn and wet-dry periods showed considerable influence in the summer (23 %). The projected change in climatic conditions will have an effect on weathering regimes efficacy and their temporal and spatial occurrence. Despite this increase of precipitation in Autumn and Winter, it is projected that this will not be enough to cover the shortfall of snow melt water (Gobiet et al., 2014) that normally sees Spring and accompanying F/T cycles as by far the biggest triggering factor (Bajni et al., 2021). Based on our experiments this could see the efficacy of these F/T cycles decrease if rock moisture drops sufficiently and is not restocked by absent snow melt water. If there is also an increase in shorter duration F/T cycles this could also see a reduction in weathering efficacy as our experiment showed sufficient time is needed for maximum effect.

5. Conclusions

In our laboratory study, we investigated different climatic stress-loading processes similar to those experienced in an alpine environment on samples of Wetterstein limestone, for the first time with a special emphasis on the role of moisture saturation. From this we were able to conclude the following:

- Rock moisture undoubtedly plays a role in limiting rock weathering processes. Through changes in rock mechanics it plays a role in when cracking events occur in these stress-loading processes.
- Regarding amounts of AE hits, long freezing (LF) is most potent followed by freeze-thaw (F/T) and warm-cold (W/C) on equal footing and wetting-drying (W/D) as last.
- The effect of frost weathering creates a similar weathering effect to that seen in temperature cycles above freezing, but at twice the thermal gradient. This would indicate that in thermal cycling of equivalent duration, subcritical crack propagation from frost weathering is similar in magnitude to a 3 K thermal gradient increase in Wetterstein limestone.

- Length of freezing cycles plays a role in efficacy. In longer freezing cycles increased moisture saturation causes at least 2× greater increase in effective porosity than dry samples and 4× as many AE hits.
- W/D has a measurable weathering effect, even if smaller than W/C and F/T. The synergistic contribution of wetting and drying to other weathering processes should not be discounted in studies, though it's overall contribution to rock degradation could be difficult to calculate as a result.
- At saturation < 25 % samples show a propensity for comparably higher energy cracking events due to rock mechanics promoting brittle deformation and AE signal energy dissipation, but not necessarily greater crack propagation.
- Moisture effect on W/C is limited. With LF, more tensile cracking occurs in more saturated samples but more re-freezing events occur at lower saturation. Also for W/D cycles most weathering occurs in the beginning of cycle phases. Therefore, the presence and mobility of pore water seem to be more important than the quantity.
- Nonetheless, the rock weathering paradigm of "the wetter the better" must be questioned, as well as the predominant role of frost weathering in alpine regions.

CRediT authorship contribution statement

Andrew Mitchell: Writing – original draft, Visualization, Methodology, Investigation, Formal analysis, Data curation, Conceptualization. **Oliver Sass:** Writing – original draft, Supervision, Resources, Project administration, Funding acquisition, Conceptualization.

Declaration of competing interest

The authors declare that they have no known competing financial interests or personal relationships that could have appeared to influence the work reported in this paper.

Data availability

Data will be made available on request.

Acknowledgements

References

Aggelis, D.G., 2011. Classification of cracking mode in concrete by acoustic emission parameters. Mech. Res. Commun. 38 (3), 153–157. ISSN 0093-6413,. https://doi.org/10.1016/j.mechrescom.2011.03.007.

Aldred, J., Eppes, M.C., Aquino, K., Deal, R., Garbini, J., Swami, S., Tuttle, A., Xanthos, G., 2016. The influence of solar-induced thermal stresses on the mechanical weathering of rocks in humid mid-latitudes. Earth Surf. Process. Landf. 41 (5), 603–614. https://doi.org/10.1002/esp.3849.

Bajni, G., Camera, C.A.S., Apuani, T., 2021. Deciphering meteorological influencing factors for Alpine rockfalls: a case study in Aosta Valley. Landslides 18, 3279–3298. https://doi.org/10.1007/s10346-021-01697-3.

Beattie, A.G., 1983. Acoustic emission, principles and instrumentation. JAcoustEmiss 2 (1/2), 95–128 url. http://www.aewg.org/jae/JAE-Vol_02-1983.pdf. (Accessed 3 June 2024).

Collins, B.D., Stock, G.M., 2016. Rockfall triggering by cyclic thermal stressing of exfoliation fractures. Nat. Geosci. 9, 395–400. https://doi.org/10.1038/NGEO2686.

Collins, B.D., Stock, G.M., Eppes, M.-C., Lewis, S.W., Corbett, S.C., Smith, J.B., 2018. Thermal influences on spontaneous rock dome exfoliation. Nat. Commun. 9 (1), 762. https://doi.org/10.1038/s41467-017-02728-1.

Cox, S.J.D., Meredith, P.G., 1993. Microcrack formation and material softening in rock measured by monitoring acoustic emissions. Int. J. Rock Mech. Min. Sci. Geomech. Abstr. 30 (1), 11–24. ISSN 0148-9062. https://doi.org/10.1016/0148-9062(93)90172-A.

Deresse, N., Van Steen, C., Sarem, M., François, S., Verstrynge, E., 2023. 'Crack mode analysis of cement mortars with signal - based acoustic emission techniques'. EWGAE35 & ICAE10 Conference on Acoustic Emission Testing, Ljubljana, Slovenia, September 2022. e-J. Nondestruct. Eval. 28 (1) https://doi.org/10.58286/27626.

Dong, W., Han, L., Meng, L., Zhu, H., Yan, S., Xu, C., Dong, Y., 2022. Experimental study on the mechanical and acoustic emission characteristics of tuff with different moisture contents. Minerals 12, 1050. https://doi.org/10.3390/min12081050.

Draebing, D., Haberkorn, A., Krautblatter, M., Kenner, R., Phillips, M., 2017. Thermal and mechanical responses resulting from spatial and temporal snow cover variability in permafrost rock slopes, Steintaelli, Swiss Alps. Permafr. Periglac. Process. 28 (1), 140–157. https://doi.org/10.1002/ppp.1921.

Du, K., Li, X., Tao, M., Wang, S., 2020. Experimental study on acoustic emission (AE) characteristics and crack classification during rock fracture in several basic lab tests. Int. J. Rock Mech. Min. Sci. 133 https://doi.org/10.1016/j.ijrmms.2020.104411. ISSN 1365-1609.

Duca, S., Occhiena, C., Mattone, M., Sambuelli, L., Scavia, C., 2014. Feasibility of ice segregation location by acoustic emission detection: a laboratory test in gneiss. Permafr. Periglac. Process. 25 (3), 208–219. https://doi.org/10.1002/ppp.1814.

Emmanuel, S., Levenson, Y., 2014. Limestone weathering rates accelerated by micron-scale grain detachment. Geology 42. https://doi.org/10.1130/G35815.1.

Eppes, M.-C., Keanini, R., 2017. Mechanical weathering and rock erosion by climate-dependent subcritical cracking. Rev. Geophys. 55, 470–508. https://doi.org/10.1002/2017RG000557.

Eppes, M.C., Magi, B., Hallet, B., Delmelle, E., Mackenzie-Helnwein, P., Warren, K., Swami, S., 2016. Deciphering the role of solar-induced thermal stresses in rock weathering. Geol. Soc. Am. Bull. 128 (9–10), 1315–1338. https://doi.org/10.1130/B31422.1.

Eppes, M.C., Magi, B., Scheff, J., Warren, K., Ching, S., Feng, T., 2020. Warmer, wetter climates accelerate mechanical weathering in field data, independent of stress-loading. Geophys. Res. Lett. 47, 2020GL089062 https://doi.org/10.1029/2020GL089062.

Eppinger, S., Krautblatter, M., Mamot, P., 2018. Frozen and saturated Wetterstein limestone – a characterisation of changing rock strength. Geophys. Res. Abstr. 20. EGU2018-16098, EGU General Assembly 2018. =url. https://ui.adsabs.harvard.edu/abs/2018EGUGA..2016098E.

Gerber, D., Wilen, L.A., Poydenot, F., Dufresne, E.R., Style, R.W., 2022. Stress accumulation by confined ice in a temperature gradient. Proc. Natl. Acad. Sci. U. S. A. 119 (31), e2200748119 https://doi.org/10.1073/pnas.2200748119.

Gilbert, G.K., 1877. Report on the Geology of the Henry Mountains. US Geographical and Geological Survey of the Rocky Mountain Region, Washington, DC. https://doi.org/10.3133/70039916.

Gobiet, A., Kotlarski, S., Beniston, M., Heinrich, G., Rajczak, J., Stoffel, M., 2014. 21st century climate change in the European Alps—a review. Sci. Total Environ. 493, 1138–1151. ISSN 0048-9697. https://doi.org/10.1016/j.scitotenv.2013.07.050.

Goszczyńska, B., 2014. Analysis of the process of crack initiation and evolution in concrete with acoustic emission testing. Arch. Civ. Mech. Eng. 14 (1), 134–143. https://doi.org/10.1016/j.acme.2013.06.002.

Grosse, C.U., Ohtsu, M., Aggelis, D.G., Shiotani, T. (Eds.), 2022. Acoustic Emission Testing: Basics for Research–Applications in Engineering. *Springer Nature*. https://doi.org/10.1007/978-3-030-67936-1. ISBN : 978-3-030-67935-4.

Guo, J., Feng, G.R., Qi, T.Y., Wang, P.F., Yang, J., Li, Z., Bai, J., Du, X., Wang, Z., 2018. Dynamic mechanical behavior of dry and water saturated igneous rock with acoustic emission monitoring. *Shock*. Vib., 2348394 https://doi.org/10.1155/2018/2348394.

Hall, K., 1991. Rock moisture data from the Juneau Icefield (Alaska), and its significance for mechanical weathering studies. Permafr. Periglac. Process. 2, 321–330. https://doi.org/10.1002/ppp.3430020407.

Hall, K., 1993. Rock moisture data from Livingston Island (Maritime Antarctic) and implications for weathering studies. Permafr. Periglac. Process. 4, 245–253. https://doi.org/10.1002/ppp.3430040306.

Hall, K., 2013. Mechanical weathering in cold regions. In: Shroder, J.F. (Ed.), Treatise on Geomorphology. Academic Press, San Diego, pp. 258–276. https://doi.org/10.1016/B978-0-12-374739-6.00062-2.

Hall, K., Thorn, C.E., Matsuoka, N., Prick, A., 2002. Weathering in cold regions: some thoughts and perspectives. Prog. Phys. Geogr. 26, 577–603. https://doi.org/10.1191/0309133302pp353ra.

Hallet, B., Walder, J.S., Stubbs, C.W., 1991. Weathering by segregation ice growth in microcracks at sustained sub-zero temperatures: Verification from an experimental study using acoustic emissions. Permafr. Periglac. Process. 2 (4), 283–300. https://doi.org/10.1002/ppp.3430020404.

Hamès, V., Lautridou, J.-P., Ozer, A., et al., 1987. 'Variations dilatométriques de roches soumises à des cycles' « humidification-séchage ». Géog. Phys. Quatern. 41 (3), 345–354. https://doi.org/10.7202/032690ar.

Hudec, P.P., Sitar, N., 1975. Effect of water sorption on carbonate rock expansivity. Can. Geotech. J. 12, 179–186. https://doi.org/10.1139/t75-022.

JCMS-IIIB5706, 2003. Monitoring Method for Active Cracks in Concrete by Acoustic Emission, Construction Materials Standard. *Federation of Construction Materials Industries*, pp. 23–28.

Jia, H., Xiang, W., Krautblatter, M., 2015. Quantifying rock fatigue and decreasing compressive and tensile strength after repeated freeze-thaw cycles. Permafr. Periglac. Process. 26 (4), 368–377. https://doi.org/10.1002/ppp.1857.

Kießl, K., 1983. 'Kapillarer und Dampff örmiger Feuchtetransport in mehrschichtigen Bauteilen'. Rechnetische Erfassung und bauphysikalische Anwendung. Dissertation. Universität-Gesamthochschule Essen.

Kodama, J., Goto, T., Fujii, Y., Hagan, P., 2013. The effects of water content, temperature and loading rate on strength and failure process of frozen rocks. Int. J. Rock Mech. Min. Sci. 62, 1–13. https://doi.org/10.1016/j.ijrmms.2013.03.006.

Krautblatter, M., Funk, D., Günzel, F.K., 2013. Why permafrost rocks become unstable: a rock-ice-mechanical model in time and space. Earth Surf. Process. Landf. 38, 867–887. https://doi.org/10.1002/esp.3374.

Levenson, Y., Emmanuel, S., 2013. Pore-scale heterogeneous reaction rates on a dissolving limestone surface. Geochim. Cosmochim. Acta 119, 188–197. https://doi.org/10.1016/j.gca.2013.05.024.

Li, C., Liu, N., Liu, W., Feng, R., 2021a. Study on characteristics of energy storage and acoustic emission of rock under different moisture content. Sustainability 13, 1041. https://doi.org/10.3390/su13031041.

Li, H., Qiao, Y., Shen, R., He, M., Cheng, T., Xiao, Y., Tang, J., 2021b. Effect of water on mechanical behavior and acoustic emission response of sandstone during loading process: phenomenon and mechanism. Eng. Geol. 294, 106386. ISSN 0013-7952. https://doi.org/10.1016/j.enggeo.2021.106386.

Li, J., Lian, S., Huang, Y., Wang, C., 2022. Study on crack classification criterion and failure evaluation index of red sandstone based on acoustic emission parameter analysis. Sustainability 14, 5143. https://doi.org/10.3390/su14095143, 2022.

Li, Z., Ma, X., Kong, X., O. Saar, M., Vogler, D., 2023. Permeability evolution during pressure-controlled shear slip in saw-cut and natural granite fractures. Rock Mech. Bull. 2 (2), 100027. ISSN 2773-2304. https://doi.org/10.1016/j.rockmb.2022.100027.

Lin, Q.B., Cao, P., Cao, R.H., Fan, X., 2019. Acoustic emission characteristics during rock fragmentation processes induced by disc cutter under different water content conditions. Appl. Sci. Basel 9 (1), 194. https://doi.org/10.3390/app9010194.

Liu, X.X., Wu, L.X., Zhang, Y.B., Liang, Z.Z., Yao, X.L., Liang, P., 2019. Frequency properties of acoustic emissions from the dry and saturated rock. Environ. Earth Sci. 78 (3), 67. https://doi.org/10.1007/s12665-019-8058-x.

Lockner, D., 1993. The role of acoustic emission in the study of rock fracture. Int. J. Rock Mech. Min. Sci. Geomech. Abstr. 30 (7), 883–899. https://doi.org/10.1016/0148-9062(93)90041-b.

Maji, V., Murton, J.B., 2021. Experimental observations and statistical modeling of crack propagation dynamics in limestone by acoustic emission analysis during freezing and thawing. J. Geophys. Res. Earth 126, e2021JF006127. https://doi.org/10.1029/2021JF006127.

Martínez-Martínez, J., Benavente, D., Gomez-Heras, M., Marco-Castaño, L., García-del-Cura, M.A., 2013. Non-linear decay of building stones during freeze–thaw weathering processes. Constr. Build. Mater. 38, 443–454. https://doi.org/10.1016/j.conbuildmat.2012.07.059.

Matsuoka, N., 2001. Microgelivation versus macrogelivation: towards bridging the gap between laboratory and field frost weathering. Permafr. Periglac. 12 (3), 299–313. https://doi.org/10.1002/ppp.393.

Matsuoka, N., 2008. Frost weathering and rockwall erosion in the southeastern Swiss Alps: long-term (1994-2006) observations. Geomorphology 99 (1–4), 353–368. https://doi.org/10.1016/j.geomorph.2007.11.013.

Mayer, T., Eppes, M., Draebing, D., 2023. Influences driving and limiting the efficacy of ice segregation in alpine rocks. Geophys. Res. Lett. 50, e2023GL102951 https://doi.org/10.1029/2023GL102951.

Meng, F., Zhou, H., Li, S., et al., 2016. Shear behaviour and acoustic emission characteristics of different joints under various stress levels. Rock Mech. Rock. Eng. 49, 4919–4928. https://doi.org/10.1007/s00603-016-1034-9.

Meng, F., Baud, P., Ge, H., Wong, T., 2019. The effect of stress on limestone permeability and effective stress behavior of damaged samples. J. Geophys. Res. Solid Earth 124, 376–399. https://doi.org/10.1029/2018JB016526.

Moss, A.J., Green, P., Hutka, J., 1981. Static breakage of granitic detritus by ice and water in comparison with breakage by flowing water. Sedimentology 28, 261–272. https://doi.org/10.1111/j.1365-3091.1981.tb01679.x.

Murton, J.B., Peterson, R., Ozouf, J.C., 2006. Bedrock fracture by ice segregation in cold regions. Science 314 (5802), 1127–1129. https://doi.org/10.1126/science.1132127.

Musso Piantelli, F., Herwegh, M., Anselmetti, F.S., Waldvogel, M., Gruner, U., 2020. Microfracture propagation in gneiss through frost wedging: insights from an experimental study. Nat. Hazards 100, 843–860. https://doi.org/10.1007/s11069-019-03846-3.

Nepper-Christensen, P., 1965. Shrinkage and swelling of rocks due to moisture movements. In: Meddelser fra Dansk Geologisk Forening, 15, pp. 548–555 url. https://2dgf.dk/xpdf/bull-1964-15-4-548-555.pdf. (Accessed 3 June 2024).

Ohno, K., Ohtsu, M., 2010. Crack classification in concrete based on acoustic emission. Constr. Build. Mater. 24, 2339–2346. https://doi.org/10.1016/j.conbuildmat.2010.05.004.

Pissart, A., Lautridou, J.-P., 1984. Variations de longueur de cylinders de Pierre de Caen (calcaire bathonien) sous l'effect de se'charge et d'humidification. Z. fur Geomorphol. 49, 111–116. https://doi.org/10.7202/032690ar. Supplement Bund.

Prick, A., 1995. Dilatometrical behaviour of porous calcareous rock samples subjected to freeze-thaw cycles. Catena 25 (1), 7–20. https://doi.org/10.1016/0341-8162(94)00038-G.

Prick, A., 1997. Critical degree of saturation as a threshold moisture level in frost weathering of limestones. Permafr. Periglac. 8 (1), 91–99. https://doi.org/10.1002/(SICI)1099-1530(199701)8:1<91::AID-PPP238>3.0.CO;2-4.

Rajczak, J., Pall, P., Schär, C., 2013. Projections of extreme precipitation events in regional climate simulations for Europe and the Alpine Region. J. Geophys. Res. Atmos. 118 (9), 3610–3626. https://doi.org/10.1002/jgrd.50297.

Ranjith, P.G., Jasinge, D., Song, J.Y., Choi, S.K., 2008. A study of the effect of displacement rate and moisture content on the mechanical properties of concrete: use of acoustic emission. Mech. Mater. 40 (6), 453–469. https://doi.org/10.1016/j.mechmat.2007.11.002.

Rode, M., Schnepfleitner, H., Sass, O., 2016. Simulation of moisture content in alpine rockwalls during freeze–thaw events. Earth Surf. Process. Landf. 41 (13), 1937–1950. https://doi.org/10.1002/esp.3961.

Sass, O., 2004. Rock moisture fluctuations during freeze-thaw cycles: preliminary results from electrical resistivity measurements. Polar Geogr. 28 (1), 13–31. https://doi.org/10.1080/789610157.

Sass, O., 2005. Rock moisture measurements: techniques, results, and implications for weathering. Earth Surf. Process. Landf. 30 (3), 359–374. https://doi.org/10.1002/esp.1214.

Sause, M., 2011. Investigation of Pencil-Lead Breaks as Acoustic Emission Sources. J. Acoust. Emiss. 29, 184–196.

Stück, H., Plagge, R., Siegesmund, S., 2013. Numerical modeling of moisture transport in sandstone: the influence of pore space, fabric and clay content. Environ. Earth Sci. 69, 1161–1187. https://doi.org/10.1007/s12665-013-2405-0.

Voigtländer, A., 2020. Controls of Progressive Rock Failure: Environmental Conditions, Subcritical Mechanisms and Rock Stress Memory. Dissertation. Technische Universität München, p. 194. url. https://nbn-resolving.de/urn/resolver.pl?urn:nbn:de:bvb:91-diss-20201026-1551893-1-7.

Voigtländer, A., Leith, K., Krautblatter, M., 2018. Subcritical crack growth and progressive failure in carrara marble under wet and dry conditions. J. Geophys. Res. Solid Earth 123 (5), 3780–3798. https://doi.org/10.1029/2017JB014956.

Walder, J.S., Hallet, B., 1985. A theoretical-model of the fracture of rock during freezing. Geol. Soc. Am. Bull. 96 (3), 336–346. https://doi.org/10.1130/0016-7606(1985)96<336:ATMOTF>2.0.CO;2.

Walder, J.S., Hallet, B., 1986. The physical basis of frost weathering - toward a more fundamental and unified perspective. Arct. Alp. Res. 18 (1), 27–32. https://doi.org/10.2307/1551211.

Wang, Y., Zhang, B., Gao, S.H., Li, C.H., 2021. Investigation on the effect of freeze-thaw on fracture mode classification in marble subjected to multi-level cyclic loads. Theor. Appl. Fract. Mech. 111, 102847. ISSN 0167-8442. https://doi.org/10.1016/j.tafmec.2020.102847.

White, S.E., 1976. Is Frost Action Really Only Hydration Shattering? A Review. Arct. Alp. Res. 8 (1), 1–6. https://doi.org/10.2307/1550606.

Xu, Junce, Hai, Pu, Sha, Ziheng, 2022. Effect of freeze-thaw damage on the physical, mechanical, and acoustic behavior of sandstone in Urumqi. Appl. Sci. 12 (15), 7870. https://doi.org/10.3390/app12157870.

Yatsu, E., 1988. The Nature of Weathering: An Introduction. Sozosha, Tokyo, 624 pp.. https://doi.org/10.1177/030913339001400119.

Zhang, D., Chen, A., Wang, X., et al., 2015. Quantitative determination of the effect of temperature on mudstone decay during wet–dry cycles: a case study of 'purple mudstone' from south-western China. Geomorphology 246, 1–6. ISSN 0169-555X,. https://doi.org/10.1016/j.geomorph.2015.06.011.

Zhang, Z., Niu, Y., Shang, Ye, P., Zhou, R., Gao, F., 2021. Deterioration of physical and mechanical properties of rocks by cyclic drying and wetting. Geofluids 15. https://doi.org/10.1155/2021/6661107 vol., Article ID 6661107.

Zhao, T., Zhang, P., Xiao, Y., et al., 2023. Master crack types and typical acoustic emission characteristics during rock failure. Int. J. Coal Sci. Technol. 10, 2. https://doi.org/10.1007/s40789-022-00562-5.

Zhou, Z.L., Cai, X., Ma, D., Cao, W.Z., Chen, L., Zhou, J., 2018. Effects of water content on fracture and mechanical behavior of sandstone with a low clay mineral content. Eng. Fract. Mech. 193, 47–65. https://doi.org/10.1016/j.engfracmech.2018.02.028.

Zhu, J., Deng, J.H., Chen, F., Huang, Y.M., Yu, Z.Q., 2020. Water saturation effects on mechanical and fracture behavior of marble. Int. J. Geomech. 20 (10), 04020191 https://doi.org/10.1061/(ASCE)GM.1943-5622.0001825.